Biomimetic Finger Control by Filtering of Distributed Forelimb Pressures

David J. Curcie, James A. Flint, and William Craelius, *Life Member, IEEE*

***Abstract*—A linear filter was developed for decoding finger commands from volitional pressures distributed within the residual forelimb. Filter parameters were based on dynamic pressures recorded from the residual limb within its socket, during specific finger commands. A matrix of signal features was derived from eight-dimensional (8-D) pressure vectors, and its pseudoinverse comprised the filter parameters. Results with amputees showed that the filter could discriminate specific finger flexion commands, suggesting that pressure vector decoding (PVD) can provide them with biomimetic finger control.**

***Index Terms*—Linear filter, prosthetic, pseudoinverse, robotic hand.**

I. Introduction

WHILE prosthetic terminal devices can be controlled with voluntary electromyographic (EMG) signals from the residual limb, their function is generally limited to one degree of freedom (DOF), i.e., grasping. A major reason for this limitation is the relative unsuitability of the EMG for joint control, since it consists of noise with little direct relationship to joint movements. Nevertheless advanced signal processing techniques continue to improve EMG-based control of prosthetic hands [1]–[5].

Alternatives to EMG-based control use muscle and tendon forces generated within the prosthetic socket. An early demonstration of this method was the *French Electric Hand*, which used pneumatic pressure generated voluntarily within the socket to actuate a 1-DOF hand [6]. More recently, Abboudi *et al.* [7] showed that many amputees could express control over independent prosthetic fingers through dynamic pressure and shape changes at specific sites on their residua. These three-dimensional mechanical dynamics can be measured with myo-pneumatic (M-P) sensors within the socket [8]. A fine degree of residual limb muscle control was also demonstrated by amputees in a study using Hall effect magnetic movement sensors [9].

Direct coupling of individual sensors to corresponding finger actuators is complicated by the fact that volitional pressure changes at specific sensor sites may not be exclusive for individual finger motions. Thus finger-tap command "impulses" with the limb are degraded through a mechanical system that includes the effector muscles, connective tissues, and the sensor-skin interface. To recover these degraded signals, a pressure vector decoder (PVD) is herein introduced that extracts multiple DOF from distributed volitional dynamics in the residual forelimb. The restored commands can control fingers in near real-time, thus restoring a degree of biomimetic dexterity to the user.

Manuscript received November 9, 1999; revised June 26, 2000, September 29, 2000, and November 30, 2000. This work was funded by an NIH STTR grant to Nian-Crae, Inc.

The authors are with the Orthotic and Prosthetic Laboratory, Department of Biomedical Engineering, Rutgers University, Piscatway, NJ 08854.

Publisher Item Identifier S 1534-4320(01)01778-8.

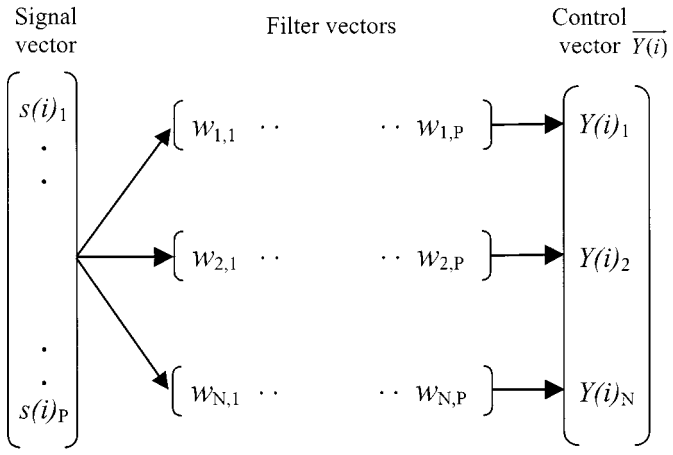

Fig. 1. Discriminatory filtering of distributed interfacial pressure data. Filtering for N fingers is shown. Filter vectors $\overrightarrow{w}_f (f = 1 \cdots N)$, comprised of custom weights, are applied to the signal vector, $\overrightarrow{s(i)}$, to obtain a control vector, $\overrightarrow{Y(i)}$, an approximation of the intended movements.

II. Methods

A. Overview of Pressure-Vector Decoding

Decoding finger commands from a spatial array of P pressure sensors involves filtering the input pressure vector, $\overrightarrow{s(i)}$, *to* obtain real-time output, $Y(i)_f$, for each of N fingers ($f = 1, \ldots, N$), (Fig. 1). $Y(i)_f$ is calculated as a function of the linear combination of instantaneous pressure vector $\overrightarrow{s(i)}$ and a filter vector $\overrightarrow{w}_f$ as follows:

$$Y(i)_f = \left| \overrightarrow{s(i)} \overrightarrow{w}_f \right|^2 = \left| \sum_{k=1}^{P} (s(i)_k \cdot w_{f,k}) \right|^2. \qquad (1)$$

Since only positive output is used for finger control, signals may be full-wave rectified (absolute value) and squared, as indicated above.

In Fig. 1, a specific set of input pressure vectors is related to a corresponding set of output vectors, $\overrightarrow{Y(i)}$, representing joint positions. Since the filter is trained by discrete movements, i.e., single finger flexions, its output relates only to those movements, and is not necessarily proportional to their intensities.

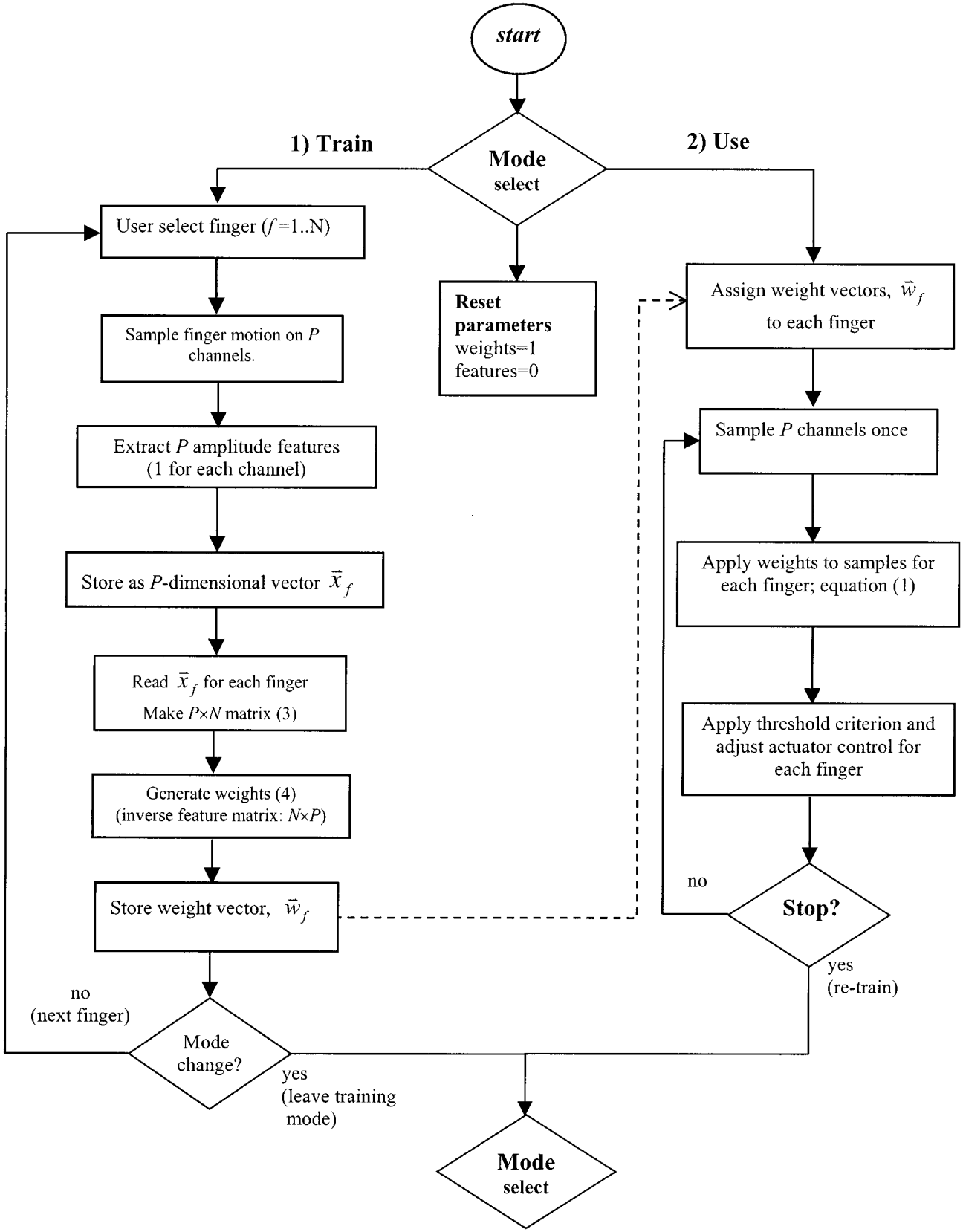

Fig. 2. Flowchart of training and control. The proposed system has two modes: train and use, switchable from the user interface.

Decoding of specific movement requests therefore involves discretization of $Y(i)_f$ with an appropriate threshold function. In the ideal case, a simple amplitude threshold for $Y(i)_f$ should decode all movement requests with complete specificity.

B. Filter Training

To optimize individual finger control, $\vec{w}_f$ for each finger is adapted for the user in a supervised training stage, as shown in Fig. 2 (left branch). Training the filter involves quantifying the degradation of the volitional commands through the limb and M-P sensor interface. First, a single amplitude feature is estimated for each channel during requested finger motions, forming a feature vector, $\vec{x}_f$. The amplitude feature represents the impulse response of a finger-tap volition, measured by the M-P sensors. An effective feature for M-P signals is the root-mean-square (rms) amplitude of a signal sequence during repeated specified movements, and is used for this study. More complete signal features can also be used. The rms amplitude is calculated using

$$x_k = \sqrt{\frac{1}{n}\sum_{i=0}^{n-1} s(i)_k^2}. \tag{2}$$

The feature vectors for each finger, $\vec{x}_f (f = 1, \ldots, N)$, form the columns of a $P \times N$ feature matrix:

$$\mathbf{H} = \begin{vmatrix} x_{1,1} & x_{1,2} & \cdots & x_{1,N} \\ x_{2,1} & x_{2,2} & \cdots & x_{2,N} \\ \vdots & & \cdots & \vdots \\ x_{P,1} & x_{P,2} & \cdots & x_{P,N} \end{vmatrix}. \tag{3}$$

$\mathbf{H}$ represents the degradation of the intended volitional commands through the residual limb and sensor interface. Its inverse restores the command impulses for the measured feature model, based on an algebraic restoration method [10], [11]. The filter $\mathbf{W}$ is the $N \times P$ discrimination matrix

$$\mathbf{W} = \mathbf{H}^{-1} = \begin{vmatrix} w_{1,1} & w_{1,2} & \cdots & w_{1,P} \\ w_{2,1} & w_{2,2} & \cdots & w_{2,P} \\ \vdots & & \cdots & \vdots \\ w_{N,1} & w_{N,2} & \cdots & w_{N,P} \end{vmatrix}. \tag{4}$$

If $\mathbf{H}$ is not square, its pseudoinverse is calculated using singular-value decomposition [11], [12]. Each of the N rows of $\mathbf{W}$ is a filter (weighting) vector, $\vec{w}_f$, representing the relative contribution of each input channel to the respective output channel f, as in (1).

The described filter may be applied to prosthetic finger control, as shown in Fig. 2 (right branch).

III. Experimental Methods

A. Data Acquisition

Results are presented from a 28-year-old male amputee, of ten years duration, with a 12-cm residuum (subject A). A second below-elbow amputee male subject (B) was also tested, who is 70 years of age, and received the injury approximately 50 years prior. Both subjects were tested following informed written consent, after approval of the study from the University Institutional Review Board. The subjects were able to perceive and attain motion control over 3 phantom fingers. This observation provided rationale for selecting a three-finger control filter. Eight locations for sensor placement were determined by palpating the forearm during volitional finger motions, as described in Abboudi *et al.* [7]. A silicone sleeve custom fit for the subject was constructed, incorporating the M-P sensors into its structure at the chosen locations (Fig. 3). A custom socket was then placed over the sleeve, tightly enclosing the limb and sensors. Six of the eight sensors were clustered around the *flexor digitorum superficialis and the flexor carpi ulnaris*, circumscribing a relatively small area of 28 cm^2.

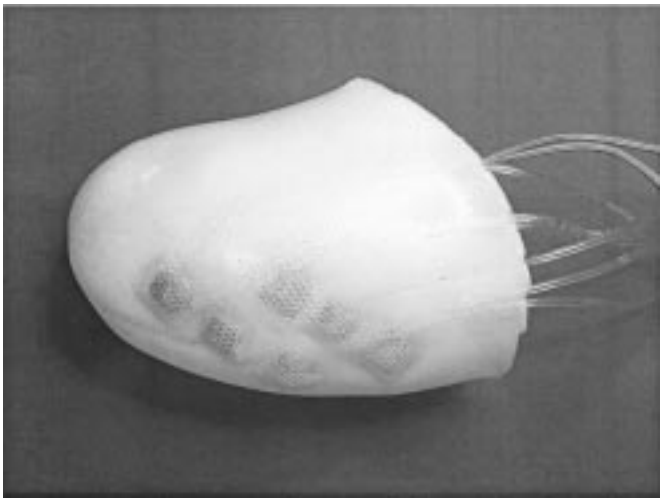

Fig. 3. Silicon sleeve with integrated M-P sensors. The sleeve for subject A is shown. Six of the eight sensors, and the pneumatic tubing are visible within the sleeve's structure.

The eight M-P sensors were connected via tubing to eight pressure transducers (Sensym SCX-01, Santa Clara, CA.), connected to an eight-channel data acquisition board (DAP/1200, Microstar Laboratories, Inc., Bellevue, WA). Data from the M-P sensors were sampled at 200 Hz per channel and 12-bits resolution, and stored to files for offline processing.

The training and control system was emulated on a PC using LabVIEW graphical programming software (National Instruments Corp, Austin, TX), and DADiSP signal processing software (DSP Development Corp, Cambridge, MA). Data were exchanged between the two applications in real-time using dynamic data exchange (DDE). For the emulation, all sensor data were recorded off-line and read into the system.

B. Protocol

The training protocol consisted of five full flexions of each of three fingers over a 4-s period (Figs. 2, 4). The phantom fingers, F1, F2, and F3, represent the thumb, middle finger, and pinky, respectively. Test data were sequential double-flexions of each of the 3 fingers, during a 12-s period [Fig. 5(a) and (b)]. Output data were displayed in a response matrix consisting of three rows, representing the output used to control each phantom finger, and three columns, representing the requested finger motions [Fig. 5(c)]. Diagonal components represent intended finger movements, while off-diagonal components represent the remaining effects of "movement cross-talk" occurring at the sensor locations. The goal of training was to

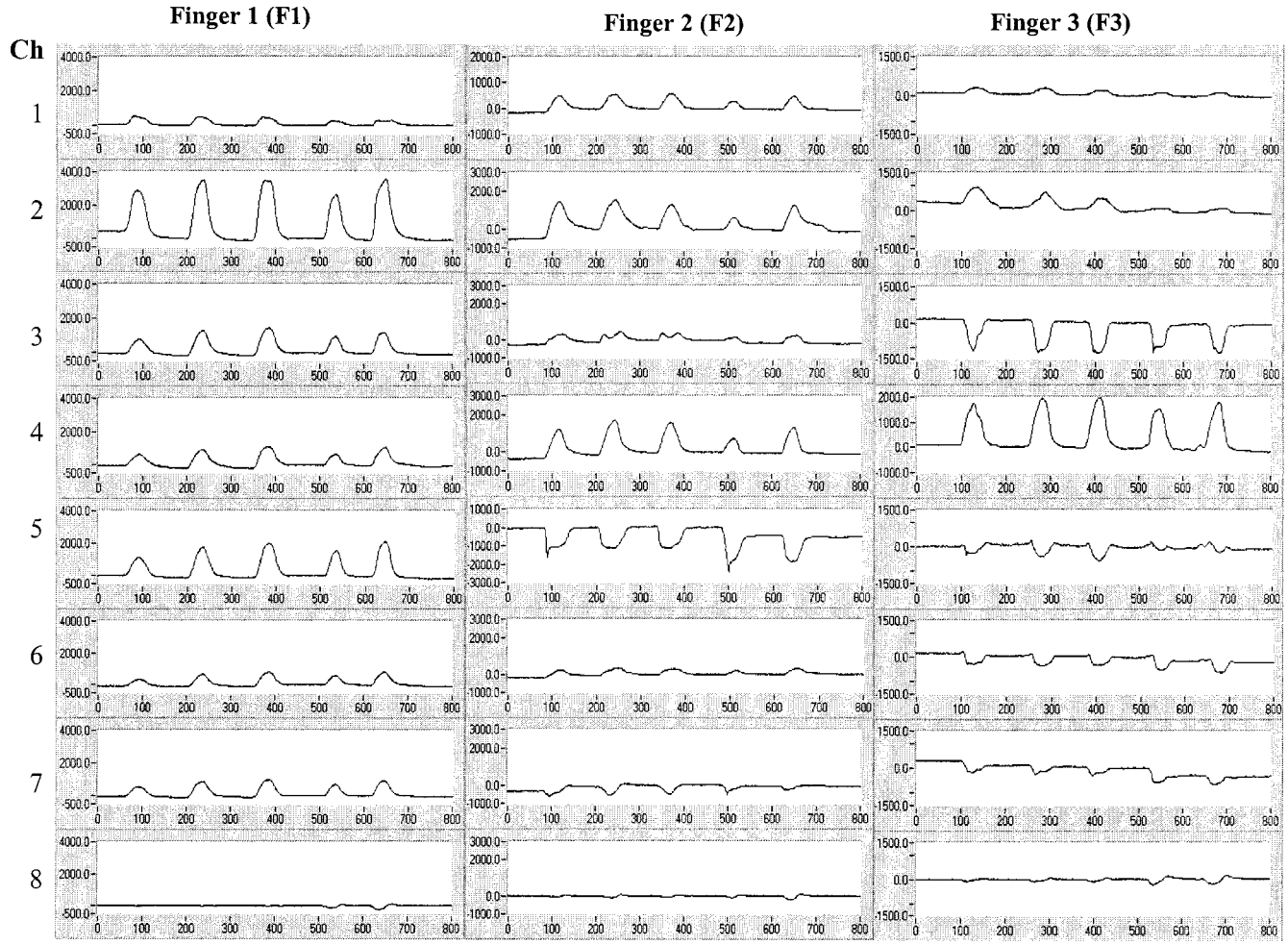

Fig. 4. Training data. This figure represents 8 channels of data, acquired for three finger volitions: the thumb (F1), middle finger (F2), and pinky (F3). The ordinate is a relative amplitude scale, and the abscissa is sample number.

maximize the signal on the diagonal, relative to the off diagonal of the response matrix.

The system was trained and tested based on two types of signal features: the peak amplitude measure from each channel, and the rms. The specificity of each feature extraction method was quantified as the ratios of the signal energies of the diagonal components over the off-diagonal components, for each finger movement sequence, according to

$$R_{ij} = 10\log\frac{\sqrt{\sum(D_i)^2}}{\sqrt{\sum(O_{ij})^2}} \qquad i, j = 1, 2, 3; i \neq j \qquad (5)$$

where the numerator is the signal energy of the diagonal component on output channel i, and the denominator is the energy of the off-diagonal components, j, on channel i. Output channel records [Fig. 5(c)] were each segmented into three even segments prior to energy calculation, to separate the diagonal and off-diagonal components.

IV. Results

Fig. 4 shows eight channels of intrasocket pressures recorded during supervised training of subject A. Records consist of five taps from each of three fingers. Upward signals represent positive pressure, due to outward movement at the M-P sensor site, while downward signals represent negative pressure due to inward movement (concavity). The amplitude of each signal thus indicates both the magnitude and sign of the mechanical deflection, whether it is a bulge or a concavity. Signal-to-noise ratio (SNR) appears high for all channels except channel 8. Comparison of signals for each finger indicates that each movement produces a visibly different signal array, although some channels show more difference than others. For example, channels 3, 5, 6, and 7 record opposite polarities for F1 and F3, suggesting a reciprocal relationship whereby F1 causes a bulge and F3 causes a concavity at these sites. Channel 1, by contrast, appears to record similar amplitudes for all motions, indicating that the region near sensor 1 is commonly activated for all movements. Channel 8 has uniformly low amplitude, indicating it is in a mechanically inactive area.

To derive a filter based on the behavior of each channel during different movements, selected features of each signal were encoded by the feature matrix (3). In this study, no attempt was made to optimize the feature matrix. For the filter shown in Table I, signal features were represented by rms values over the entire 5-tap sequence, producing the weights listed. As expected

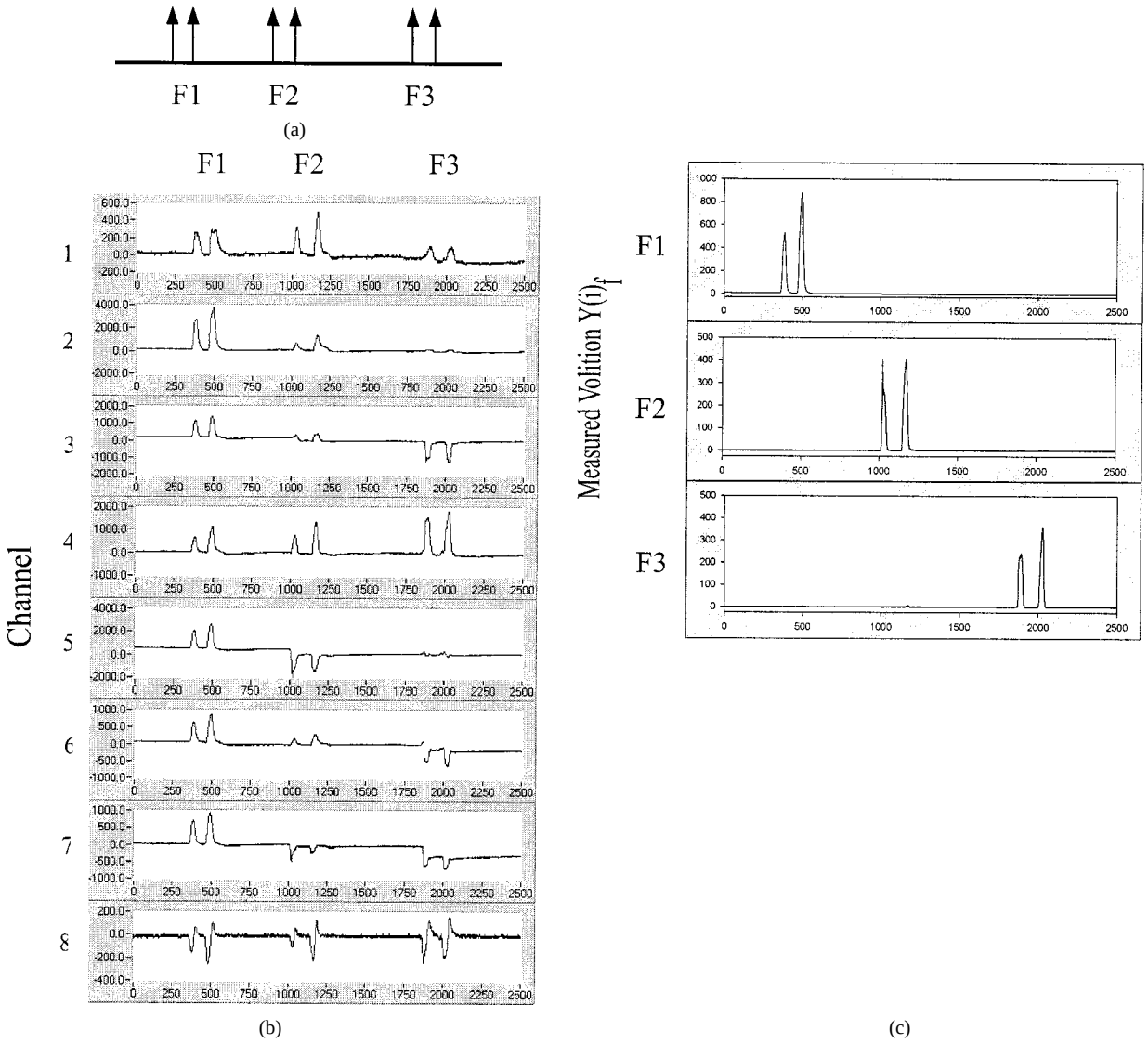

Fig. 5. Pressure vector decoding of M-P data. (a) Intended volition. The test set was two taps on each of three fingers, sequentially, sampled on 8 channels. (b) Test input data. Shown are 12.5 s of data at a sampling rate of 200 Hz. Axes are the same as Fig. 4. Note: amplitude scale varies among channels, and differs from Fig. 4. (c) Output signal response matrix. Traces represent 12.5 s of data, calculated from (1), including squaring and full-wave rectification. Rows represent the finger control output, and columns represent the intended volitional command.

TABLE I
RMS FEATURES AND WEIGHTS. FEATURES ARE SCALED AS RMS/100 mV^2. SIGN IS DETERMINED BASED ON THE GREATER DEVIATION ABOVE OR BELOW THE SIGNAL MODE (BASELINE). THE FEATURE VARIANCES ACROSS THE THREE MOVEMENTS ARE GIVEN. WEIGHTS ARE SHOWN SCALED TO AN ABSOLUTE MAXIMUM OF 1.0

Ch	Features				Weights		
	F1	F2	F3	var	F1	F2	F3
1	1.85	1.98	0.98	0.3	0.05	0.18	0.00
2	13.84	5.45	3.66	29.5	0.53	0.32	0.01
3	4.91	1.86	-4.42	22.6	0.28	0.46	-0.89
4	3.60	5.37	7.42	3.7	-0.02	0.22	0.77
5	7.05	-7.33	-1.48	52.3	0.46	-1.00	0.11
6	2.86	1.30	-2.29	7.0	0.16	0.28	-0.48
7	3.19	-1.84	3.50	9.0	0.12	-0.51	0.61
8	-0.47	-0.46	-0.61	.01	-0.01	-0.02	-0.06

from the visual comparisons, and their low feature variances, weights for channels 1 and 8 were relatively low, representing their low discriminatory value.

The filter derived above was tested by subject A, who voluntarily tapped each phantom finger twice in sequence, resulting in the raw input data shown in Fig. 5(b) (Note that scale differs from that of Fig. 4, i.e., channel 8 is magnified by approximately an order of magnitude relative to Fig. 4). Complete specificity on any channel for a particular movement would be realized as a measurable signal for that finger (i.e., F1), with zero signal amplitudes for the other two (i.e, F2 and F3). Comparing finger movements for each channel, it is evident that channels 2 and 7 provide some degree of specificity for F1 movements, though some cross- talk exists on channel 2 with F2 (positively), and on channel 7 with both F2 and F3 (negatively). Little specificity is seen for F2 or F3 movements on any channel.

The filtered output [Fig. 5(c)] shows that all 6 movement requests were successfully decoded by the filter with a high degree of specificity, as seen by the large diagonal signals and near zero off-diagonal signals. These relative magnitudes quantify the specificity of the filter using (5), but are not necessarily re-

TABLE II
COMPARISON OF FEATURE EXTRACTION METHODS. VALUES ARE SHOWN IN dB, ACCORDING TO (5), CALCULATED FOR SUBJECT A, AND REPRESENT THE LOG SIGNAL ENERGY OF DIAGONALS IN RELATION TO OFF-DIAGONAL COMPONENTS. THE OVERALL SCORE IS REPRESENTED BY THE SUM. HIGHER VALUES REPRESENT GREATER SPECIFICITY FOR VOLITIONAL MOVEMENTS

	Peak Amplitude	RMS
R_{12}	7.8	10.0
R_{13}	11.6	8.8
R_{21}	9.7	5.4
R_{23}	10.2	12.7
R_{31}	10.9	11.9
R_{32}	6.9	9.6
Sum	57.1	58.4

lated to volitional magnitude of movement. Although this filter is based on rms features, the maximum-amplitude feature produced similar results (see Table II), indicating that the two feature extraction methods have approximately equal discriminatory abilities for this subject. As indicated in Fig. 2 (right), final decoding of discrete movement requests can be done by amplitude thresholding the output. Similar results were obtained from subject B.

V. DISCUSSION

A. Comparison with Previous Methods

Our results suggest that specific motor commands can be decoded from the pressure vector expressed within the residual limbs of below-elbow amputees. To demonstrate this, a filter was trained to associate finger movement requests with distributed pressures measured within the prosthetic socket. The PVD filter is based on the pseudoinverse of a measured feature matrix; somewhat analogous filtering techniques have been successfully applied to image processing [10], [13] and audio source separation [14].

The PVD method of biomimetic finger control differs fundamentally from the tendon-activated pneumatic (TAP) method [7], in which individual sensors were coupled with specific fingers. The TAP method assumes that each DOF is expressed at a single site on the limb. TAP performance is, therefore, highly dependent upon accurate sensor placement and specific, high resolution movements at each sensor site. In contrast, the PVD method extracts volitional information from a spatially distributed array of sensors, relaxing the dependence upon site specificity. PVD thus offers a more robust and reliable controller, and potentially control over more DOF.

Previous methods have been described to control prosthetic upper limbs using EMG signals from one or more sites on the upper body [1]–[5]. These methods can give the user control over basic limb movements, such as elbow flexion and wrist pronation, but have not controlled fingers. The difficulty in decoding joint movement requests from EMGs lies in the fact that they are asynchronous electrical pulses from many muscle fibers and the mechanical resultant on individual motions is generally unpredictable. The PVD method is more suitable for dexterity control since the pressure vector is the final resultant of multiple motor pathways involved in specific joint movements.

B. Potential and Limitations of PVD Method

The present study is limited to decoding specified movements, namely fixed-pattern tapping. For example, the output shown in Fig. 5(c) could actuate a preprogrammed tapping motion, but could not indicate its force or velocity, since these variables were not included in training. Preliminary evidence and previous results [7], [8] have nevertheless suggested that, with proper sensor placement, degrees of proportional control can indeed be expressed by the PVD filter output. Implementing proportional control of either velocity or force will require new training protocols that include graded magnitudes of volition. Consequently, the complexity of the PVD method will increase in proportion to the resolution desired.

In limited testing of amputees under controlled conditions, the filter was easily trained and successfully controlled flexion of three phantom fingers. Our testing was done in a mostly static, unloaded arm position, and the performance of the PVD method in real-life conditions remains unproven. The PVD method may perform relatively well in the presence of such interference, however, compared with EMG based methods. First, interfacial motion artifact due to sensor-skin sliding is small, since the M-P sensors are tightly apposed to the skin with a silicone sleeve, and there is no electrical noise at the sensors. Moreover, moisture-induced artifacts are eliminated. Second, static loading effects on the M-P signal are much less severe than on the EMG, which becomes continuously and globally contaminated with high frequency noise, whereas the pressure signals remain static. Third, the simplicity of the PVD method facilitates its training under a variety of conditions. For example, distinguishing individual finger taps from various common motions such as wrist pronation and hand grasping can be done by the filter, since they have distinctive signal patterns [7] and training the filter to discriminate various motions is straightforward. Discrimination can be further optimized using systematic mechanical mapping of limb dynamics to determine optimal sensor sites [8].

C. Filter Training and Validity

The PVD filter is derived from the pseudoinverse of the M-P feature matrix that is trained by the user to recognize specific motions. The number of possible DOF depends upon the separability of the available training data, which is influenced not only by the technical performance of the sensing and decoding system, but also by the user's ability to produce distinctive pressure patterns within the socket for each movement. The subjects tested appear to have adequate ability to produce distinctive pressure patterns for the reliable discrimination of at least three DOF [7], despite variable limb conditions and the presence of damaged tissues. Performance could no doubt be improved with practice and exercise, since residual muscles are subject to atrophy.

Since prostheses are removed daily, and limbs change constantly, the filter coefficients may require frequent retraining as sensors are re-aligned or as muscles change. Such re-training would require about 10 s per finger, and actual computation time for calculation of features and filter weights is less than 100 ms on a Pentium 400 MHz computer. Thus, recalibration of the hand could be done conveniently as needed. During use (Fig. 2,

right branch), the processing time for sensor-input data and generation of each output channel, as in (1), is 20 μs per sample. Near real-time control of several prosthetic fingers using a mobile microcontroller thus appears possible.

ACKNOWLEDGMENT

The authors thank N. Newby, Ph.D., for programming advice, R. L. Abboudi, PhD., and S. L. Phillips for fabricating the sensors and sleeve, and M. Kogan, CP, for clinical consulting.

REFERENCES

[1] W.-J. Kang, J.-R. Shiu, J.-S. Lai, H.-W. Tsao, and T.-S. Kuo, "The application of cepstral coefficients and maximum likelihood method in EMG pattern recognition," *IEEE Trans. Biomed. Eng.*, vol. 42, pp. 777–784, Aug. 1995.

[2] R. Okuno, M. Yoshida, and K. Akazawa, "Development of biomimetic prosthetic hand controlled by electromyogram," in *Int. Workshop Advanced Motion Control*, vol. 1, 1996, pp. 103–108.

[3] G.-C. Chang, W.-J. Kang, J.-J. Luh, C.-K. Cheng, J.-S. Lai, J.-J. Chen, and T.-S. Kuo, "Real-time implementation of electromyogram pattern recognition as a control command of man-machine interface," *Med. Eng. Phys.*, vol. 18, no. 7, pp. 529–537, 1996.

[4] P. J. Gallant, E. L. Morin, and L. E. Peppard, "Feature-based classification of myoelectric signals using artificial neural networks," *Med. Biol. Eng. Comput.*, vol. 36, no. 4, pp. 485–489, 1998.

[5] S.-H. Park and S.-P. Lee, "EMG pattern recognition based on artificial intelligence techniques," *IEEE Trans. Rehab. Eng.*, vol. 6, pp. 400–405, Dec. 1998.

[6] L. F. Lucaccini, P. K. Kaiser, and J. Lyman, "The French electric hand: Some observations and conclusions," *Bull. Prosthetics Res.*, vol. 10, no. 6, pp. 31–51, 1966.

[7] R. L. Abboudi, C. A. Glass, N. A. Newby, J. A. Flint, and W. Craelius, "A biomimetic controller for multifinger prosthesis," *IEEE Trans. Rehab. Eng.*, vol. 7, pp. 121–129, June 1999.

[8] S. L. Phillips, R. L. Abboudi, M. Kogan, D. J. Curcie, J. A. Flint, N. A. Newby, and W. Craelius, "A smart interface for a biomimetic upper limb prosthesis," in *Proc. 6th World Biomaterials Congr.*, May 2000, p. 1343.

[9] L. P. J. Kenney, I. Lisitsa, P. Bowker, G. H. Heath, and D. Howard, "Dimensional change in muscle as a control signal for powered upper limb prostheses: A pilot study," *Med. Eng. Phys.*, vol. 21, no. 8, pp. 589–597, 1999.

[10] R. Gonzalez and P. Wintz, "Image restoration," in *Digital Image Processing*. Reading, MA: Addison-Wesley, 1979, pp. 183–207.

[11] R. W. Hendler and R. I. Shrager, "Deconvolutions based on singular value decomposition and the pseudoinverse: A guide for beginners," *J. Biochem. & Biophys. Meth.*, vol. 28, no. 1, pp. 1–33, 1994.

[12] G. Strang, "The singular value decomposition and the pseudoinverse," in *Linear Alg. Appl.*. Fort Worth, TX: Harcourt Brace Jovanovich, 1988, pp. 443–451.

[13] J. Shen and E. S. Ebbini, "Filter-based coded excitation system for high-speed ultrasonic imaging," *IEEE Trans. Med. Img.*, vol. 17, pp. 923–934, June 1998.

[14] S. M. Kuo and G. H. Canfield, "Dual-channel audio equalization and cross talk cancellation for 3-D sound reproduction," *IEEE Trans. Consumer Electron.*, vol. 43, pp. 1189–1196, Nov. 1997.

David J. Curcie received the B.S., M.S., and Ph.D. degrees in biomedical engineering from Rutgers, the State University of New Jersey, Piscataway, NJ, in 1991, 1994, and 1999, respectively. His doctoral work focused on physiological recognition based on heart rate patterns.

He continued as a Postdoctoral Fellow in the Orthotics and Prosthetics Laboratory in the Biomedical Engineering Department at Rutgers. He is employed as an Instrumentation Development Consultant for Nian-Crae, Inc., Somerset, NJ, and Creatone, Inc., Mountainside, NJ. His primary interests include physiological signal processing, pattern recognition, biometrics, and biomedical instrumentation/software development.

James A. Flint received the B.S. degree in applied science in engineering from Rutgers, the State University of New Jersey, Piscataway, NJ, in 1997. That same year he returned to Rutgers for graduate study in Biomedical Engineering. He is currently pursuing a Ph.D. degree in the area of medical instrumentation and is employed at Ethicon Inc., a Johnson & Johnson company, Somerville, NJ. His professional interests include microcontroller-based device development, signal processing, and motion control systems.

William Craelius (M'82–LM'92) received the B.S. degree in mechanical analysis and design from the University of Illinois, Urbana, in 1969, and the M.S. and Ph.D. degrees (in environmental health engineering and biomedical engineering, respectively) from Northwestern University, Evanston, IL.

He is currently Director of the Orthotics and Prosthetics Laboratory and Training Program at Rutgers University, NJ.

Dr. Carelius received a National Service Award from the National Institute of Health (NIH) for Postdoctoral work in neurophysiology at Stanford University, Stanford, CA.